

Article

Direct Electrochemical Analysis in Seawater: Evaluation of Chloride and Bromide Detection

Yuqi Chen  and Richard G. Compton *

Physical & Theoretical Chemistry Laboratory, University of Oxford, Oxford OX1 3QZ, UK; yuqi.chen@sjc.ox.ac.uk
* Correspondence: richard.compton@chem.ox.ac.uk; Tel.: +44-(0)-1865-275957; Fax: +44-(0)-1865-275410

Abstract: Chloride and bromide are two of the most abundant anions found in seawater, and knowledge of their concentrations is essential for environmental monitoring. However, the analysis of chloride and bromide in seawater is challenging due to the complex nature of the seawater matrix. From an electrochemical perspective, we investigate the suitability of three types of electrode (Au, glassy carbon and Pt) for the analysis of Cl^- and/or Br^- in seawater. With the understanding of their electrochemical behaviours in artificial seawater (ASW), optimal voltammetric procedures for their detection are developed. The results show that the Au electrode is unsuitable for use as a Cl^- and/or Br^- sensor due to its dissolution and passivation in ASW. The use of glassy carbon resulted in poorly defined chloride and bromide signals. Finally, platinum was found to be a good candidate for chloride detection in artificial seawater using square wave voltammetry, and the results obtained in natural seawater via electrochemical measurement were in good agreement with those obtained via ion chromatography. Platinum electrodes are also recommended for bromide analysis.

Keywords: electrochemical analysis; electrochemical sensor; platinum electrode; glassy carbon electrode; gold electrode; chloride quantification; bromide quantification; amperometry; seawater

1. Introduction

Water scarcity is a worldwide concern, while climate change exacerbates the water shortage problem [1]. As seawater consists of 96.5% of all known water on the earth and covers 71% of Earth's surface [2], desalinated seawater is a promising solution to the freshwater shortage, and has been implemented in the Near and Middle East, North Africa, North America and in Mediterranean countries [3]. Meanwhile, noting that the main chemicals in resultant concentrated seawater, such as salt (sodium chloride), magnesium, potassium and bromine, are basic raw materials for the chemical industry, extracting these highly concentrated and stable chemicals from concentrated seawater reduces energy consumption and makes comprehensive use of natural resources [4,5]. In this context, to maximise efficiency and utility, an important step is measuring the concentration of targeted ions in seawater before desalination. More generally, it is also meaningful to analyse the compounds in seawater, which reveals the local environment, geology and potential impact on humans. Chloride and bromide are the two anions addressed in this paper.

As shown in Table 1, chloride is the most concentrated anion in seawater. The concentration of chloride has been defined as 'chlorinity' [6,7], and it is so dominant that it was originally used to estimate salinity (the total salts dissolved in seawater) [8]. Salinity is an indicator of the ocean ecosystem, as the relative salt concentration within the body of a creature living in the sea versus the water is what determines the direction of osmotic pressure and the ease of water absorbed into or removed from the body [9]. Meanwhile, measuring the specific chloride level in natural seawater systems is also necessary for both environmental studies and corrosion science. First, toxic substances such as Hg (0) and silver nanoparticles (AgNPs) are more prone to oxidation in the presence of a high concentration of chloride, leading to soluble compounds [10–13]. Secondly, marine chloride can



Citation: Chen, Y.; Compton, R.G. Direct Electrochemical Analysis in Seawater: Evaluation of Chloride and Bromide Detection. *Chemosensors* **2023**, *11*, 297. <https://doi.org/10.3390/chemosensors11050297>

Academic Editor: Matiar R Howlader

Received: 21 April 2023

Revised: 8 May 2023

Accepted: 16 May 2023

Published: 18 May 2023



Copyright: © 2023 by the authors. Licensee MDPI, Basel, Switzerland. This article is an open access article distributed under the terms and conditions of the Creative Commons Attribution (CC BY) license (<https://creativecommons.org/licenses/by/4.0/>).

directly lead to metal corrosion [14,15], which is a major ongoing challenge in shipbuilding and maritime transport.

Bromine is an essential chemical with wide applications, such as insecticides, flame retardants, refrigerants, photosensitive materials and oilfield mining [16]. About 99% of bromine on Earth exists in the form of Br^- in seawater [17], and bromide is one of the most concentrated anions in seawater (Table 1) [18]. With seawater containing about 89 trillion tonnes of bromine [19], it is one of the main sources of bromine, the extraction of which needs to be informed by measurements of the local concentrations of bromide in seawater. Meanwhile, a key step in seawater desalination is also to remove bromide and check its concentration in the resultant water, because it is toxic and carcinogenic [20]. In addition, as the local concentrations of chloride and bromide depend on location and season [21,22], the ratio between them in normal seawater is used to monitor pollution from agricultural and industrial sources [23,24]. However, the levels of chloride are hundreds of times higher than those of bromide by weight in natural seawater [25,26], which can lead to challenges in the determination of Br^- [27,28]. Thus, it is necessary to develop methods that can measure Cl^- and/or Br^- sensitively and selectively in authentic seawater.

Table 1. Concentrations of major ions in surface seawater [18].

Ion	Molar Concentration/mM
Na^+	4.81×10^2
Mg^{2+}	5.41×10^1
Ca^{2+}	1.05×10^1
K^+	1.05×10^1
Sr^{2+}	9.20×10^{-2}
Cl^-	5.59×10^2
SO_4^{2-}	2.89×10^1
HCO_3^-	1.89
CO_3^{2-}	1.89×10^{-1}
Br^-	8.63×10^{-1}
B(OH)_4^-	8.39×10^{-2}
B(OH)_3	3.42×10^{-1}
F^-	7.00×10^{-2}

As reported by Guo et al. [10], there are several well-established methods to measure the chloride level in seawater. Traditionally, the argentometric method (Mohr's method) [29,30] and colourimetry using potassium chromate to indicate the endpoint of adding silver nitrate [31] are applied for neutral solutions. Meanwhile, potentiometric titration using silver nitrate [32–34] is considered to be easier and more precise than the colourimetric method, but both involve large sample volumes and toxic chemicals. Thus, instrumental rather than wet methods are currently commonly used for the measurement of chlorinity (Cl , g kg^{-1}). Notably, a salinometer based on the electrical conductivity of seawater, together with temperature, provides salinity (S) readings. To be more specific, S is calculated from the ratio of the conductivity of seawater to that of a KCl solution (32.4356 g/kg), with both measurements made at 15°C and under one-atmosphere pressure [7,35–37]. It can then be converted to chlorinity using the Knudsen equation (Equation (1)) [6].

$$S \left(\text{g Kg}^{-1} \right) = 1.80665 \text{Cl} \left(\text{g Kg}^{-1} \right) \quad (1)$$

However, there is necessarily a lack of accuracy, as it is an estimated value depending on salinity that primarily indicates the overall ion concentration rather than the chemical composition [7,35]. For bromide quantification, there are several techniques available, e.g., kinetic spectrophotometry [38–45], chromatography [46,47], capillary electrophoresis [48–52] and electrochemistry [53–56], but they have drawbacks from different perspectives, which have been discussed by Chen et al. [57]. In brief, kinetic spectrophotometry may not be ideal for natural samples, as the oxidising agent could react with other ions present [38,43]

and dilution of the sample is required [38]. Although chromatography and capillary electrophoresis can result in relatively accurate quantification, they are costly and time-consuming in terms of the equipment, sample preparation (dilution) and analysis [41,58].

Electrochemistry provides the benefits of robust, low-cost and simple instrumentation with competitive selectivity and sensitivity, which makes it a good analytical method for bromide and chloride quantification. Although potentiometry has been widely applied as an electrochemical technique [53–56,59,60], the complexity of electrode fabrication [54] and the logarithmic relationship between potential and the analyte make it challenging to deliver a precise and sensitive detection. Meanwhile, for existing potentiometric measurements, selectivity, especially for bromide detection with the presence of chloride at hundreds of times the level in seawater, remains a challenge [53,54]. Indication of the misfunction of potentiometric electrodes is another essential requirement that cannot be easily met. Thus, amperometry is a technique that can avoid the drawbacks of potentiometry mentioned above [61–65], but traditionally has required analytes with a low concentration so that seawater cannot be directly used. Nevertheless, these problems have recently been solved by Guo et al. [10] and Chen et al. [57], with the first two bespoke reagent-free amperometric sensors being proposed for chloride and bromide sensing, respectively, in authentic seawater.

In this paper, we assessed, compared and contrasted different electrode materials for the direct analysis of Cl^- and/or Br^- in seawater. Three electrodes, made of Au, glassy carbon and Pt, were investigated, and the full voltametric responses seen in undiluted seawater were described and analysed to understand their fundamental (electro-)chemistry using both artificial seawater (ASW) and natural seawater (NSW). The implications for the electrochemical detection of bromide and chloride were assessed, and through optimal voltametric procedures, we identified two anions of interest.

2. Experimental Section

2.1. Chemicals and Reagents

Deionised water with a resistivity of 18.2 M Ω cm at 298 K (Millipore, Millipak Express 20, Watford, UK) was utilised to prepare all synthetic solutions. All the chemicals used in the experiments were of analytical grade [66]. Artificial seawater (ASW, pH = 8.1) was prepared using the composition shown in Table 2. For the chemicals used for ASW, sodium bicarbonate (NaHCO_3 , 99.7%) was purchased from Acros Organics, UK, whereas sodium chloride (NaCl , 99.5%), potassium chloride (KCl , 99.5%), magnesium chloride dihydrate ($\text{MgCl}_2 \cdot 6\text{H}_2\text{O}$, 99.0%), calcium chloride dihydrate ($\text{CaCl}_2 \cdot 2\text{H}_2\text{O}$, 99.0%), strontium chloride hexahydrate ($\text{SrCl}_2 \cdot 6\text{H}_2\text{O}$, 99.0%), sodium sulphate (Na_2SO_4 , 99.0%), potassium bromide (KBr , 99.0%), sodium fluoride (NaF , 99.0%) and boric acid (H_3BO_3 , 99.5%) were purchased from Sigma-Aldrich, UK. The “blank” solution with the same ionic strength as seawater [66] was prepared using sodium nitrate (NaNO_3 , $\geq 99.5\%$), procured from Merck KGaA, Germany.

Table 2. Chemical composition of synthetic seawater [66].

Composition	Molar Concentration (mol dm^{-3})
NaCl	4.20×10^{-1}
KCl	9.39×10^{-3}
$\text{MgCl}_2 \cdot 6\text{H}_2\text{O}$	5.46×10^{-2}
$\text{CaCl}_2 \cdot 2\text{H}_2\text{O}$	1.05×10^{-2}
$\text{SrCl}_2 \cdot 6\text{H}_2\text{O}$	6.38×10^{-5}
Na_2SO_4	2.88×10^{-2}
NaHCO_3	2.38×10^{-3}
KBr	8.40×10^{-4}
NaF	7.15×10^{-5}
H_3BO_3	4.85×10^{-5}

2.2. Electrochemical Apparatus and Methods

Electrochemical measurements were conducted using a μ Autolab II potentiostat made by Metrohm-Autolab BV in Utrecht, Netherlands. The experiments were performed using a standard three-electrode set-up at a constant temperature of 25.0 ± 0.2 °C in a Faraday cage. The reference and counter electrodes were a mercury–mercurous sulphate electrode (MSE +0.64 V vs. SHE, BASi, West Lafayette, IN, USA) and a graphite rod in all experiments. Three different working electrodes were used, namely, a gold macro-electrode (diameter of 1.60 ± 0.01 mm, geometric area of 0.02 cm², BASi, West Lafayette, IN, USA), a glassy carbon macro-electrode (GCE, diameter of 3.00 ± 0.01 mm, geometric area of 0.07 cm², BASi, West Lafayette, IN, USA) and a platinum macro-electrode (diameter of 1.66 ± 0.01 mm, geometric area of 0.02 cm², BASi, West Lafayette, IN, USA). Before each use, the working electrode was polished with 1.0, 0.3 and 0.05 μ m alumina lapping compounds from Bucher, Germany. To remove oxygen from the solutions before electrochemical measurements, high-purity N₂ flow from BOC Gases plc, UK was used as needed. Cyclic voltammetry (CV) was conducted to investigate the electrochemical behaviour of the three working electrodes in ASW. Then, for the quantification of either bromide or chloride in ASW and/or natural seawater, square wave voltammetry (SWV) was applied.

2.3. Sample Collection and Ion Chromatography Analysis

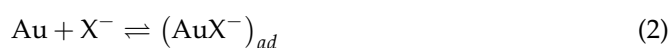
There were two authentic seawaters used in this study, and the collection of these is described by Chen et al. [57]. Ion chromatography analysis was conducted using a Dionex (Thermo Scientific, Sunnyvale, CA, USA) ICS-5000+ SP instrument, utilising a Dionex IonPac AS23-4 μ m analytical column for the separations. Before analysis, two seawater samples were each mixed with deionised water with a resistivity of 18.2 M Ω cm at 298 K at a dilution factor of 200.

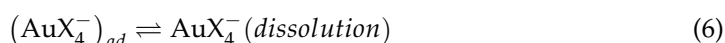
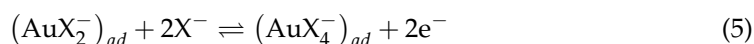
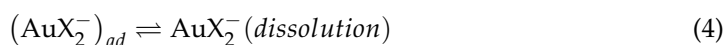
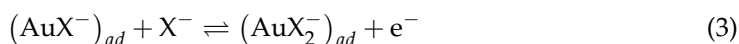
3. Results and Discussion

In the following sections, the electrochemical behaviour of the gold electrode in ASW is first reported and interpreted using observations from pure chloride and bromide solutions reported in the literature. The inferred dissolution of gold in halide solutions is concluded to make Au a less-than-optimal electrode material. Thus, glassy carbon electrodes (GCEs) and Pt electrodes are then considered as alternatives for Cl[−] and/or Br[−] detection in ASW. In addition to using cyclic voltammetry to assess the merits of the two electrodes as sensors, square wave voltammetry is also attempted/implemented to enhance their sensitivity, focussing particularly on using the GCE towards Br[−] and the Pt electrode towards Cl[−], leading to recommendations for the optimal electrode for and approach to each of the two ions. Finally, a bespoke method using a Pt electrode for chloride sensing is applied for quantitative analysis in two samples of natural seawater, while ion chromatography is conducted for validation of the measurements.

3.1. Cyclic Voltammetric Study of a Au Electrode in ASW

The electrochemical behaviour of a Au electrode in simple halide solutions has been widely studied since the last century [67–69], not least since gold is a noble metal, and methods of extracting, refining, electroplating, electro-etching and electropolishing it have been developed and optimised. As summarised by Nicol [68], chloride and bromide are two ligands that, when present at the millimolar level, coordinate with gold cations and decrease the potential for gold electro-solubilisation in acidic conditions [67,68]. To be specific, during anodic voltammetric scanning in solutions containing 0.1 M HClO₄[−] with either 10 mM Cl[−] or Br[−], respectively, the oxidation of Au occurred at similar potentials, ca. 1.0 V vs. SCE, with the voltammetric peaks attributed to the conversion of Au into Au (I) or Au (III) [67]. The general mechanism of the electrochemical dissolution of gold in halide solutions is shown below [67,70]:





where X represents Cl or Br. It is worth mentioning that the voltametric peak in perchloric acid corresponding to the oxidation of gold to AuCl_2^- or AuBr_2^- significantly overlapped the peak for AuCl_4^- or AuBr_4^- , respectively, and the relative amounts of Au(I) and Au(III) formed during oxidation was reported to be hard to determine [67,68,70–72]. Meanwhile, passivation due to the formation of an oxide film was also observed in both halide solutions, at sufficiently positive potentials which were dependent on the pH of the solutions [67,69,71,73,74]. From the perspective of sensing, the similarity between chloride and bromide presents a significant challenge in terms of selectivity using a gold electrode. Secondly, the unclear mechanism and corresponding species at different stages, namely the dissolution and passivation of gold, make it hard to develop a reliable understanding of the development of a sensor. Moreover, detection in seawater, which presents a much more complex matrix, may be expected to involve further difficulty and uncertainty. Nevertheless, in the following, we report the electrochemical behaviour of gold electrodes in seawater, ultimately leading to confirmation of the conclusion that Au is a poor choice as a Cl^- and/or Br^- sensor.

We next turn to experiments on the voltammetry at a gold electrode in seawater where chloride is present at the hundred milli-molar level and the bromide concentration is typically less than 1 mM. Cyclic voltammetric experiments were conducted using a Au electrode in three degassed artificial seawater (ASW) samples (Figure 1). ASW1 contained 0.571 M chloride and 0.84 mM bromide (black line); ASW2 contained 0.484 M chloride and 0.84 mM bromide (blue line); and ASW3 contained 0.571 M chloride and 1.84 mM bromide (green line). Note that for synthetic seawater, the recommended chloride level is in the range of 0.484 M–0.593 M [10,75,76] and the recommended bromide level is 0.84 mM [75]. The potential sweep started at -0.45 V vs. MSE, and swept towards 0.94 V before returning to -0.45 V at a scan rate of 20 mVs^{-1} .

For ASW1, the voltammetry in Figure 1 shows a large anodic peak with a peak potential of 0.90 V vs. MSE, followed by abrupt passivation on the forward voltametric scan. The peak is seen to have a shoulder at ca 0.59 V vs. MSE. The abrupt decrease in signal is attributed to the formation of gold oxide on the electrode surface, inhibiting further electron transfer. The main peak and the shoulder are tentatively assigned to the oxidation of Au to AuCl_4^- and AuBr_4^- , and also possibly to the hidden oxidation to AuCl_2^- and AuBr_2^- , described by Equations (2)–(6) [67,70]. The dissolved gold was observed to be partly plated onto the surface of the counter-electrode (Figure S1, Supporting Information Section S1) and led to colouration of the solution (Figure S2, Supporting Information Section S1) after 20 repeats of the scan, confirming the dissolution of the gold electrode, which would be a serious demerit in terms of its use as a sensor. On changing the scan direction from anodic to cathodic, a small anodic Peak 2 was observed at 0.62 V vs. MSE due to partial de-passivation following a loss of material via dissolution during the reverse scan. On continuing to scan reductively, a broad peak (Peak 3) with splitting appears at ca. -0.1 V vs. MSE, and is thought to be related to the solubilisation of the gold electrode. The other two solutions shows qualitatively analogous responses, as seen in Figure 1. Comparison of the voltammograms measured using the three different solutions suggests that the large peak is chloride-related, with the size of the signal qualitatively (but not quantitatively) increasing with the chloride levels. Note that because of the potential and concentration

competition between chloride-driven electro-dissolution of the gold and the formation of gold oxide, no simple linear relationship is expected, nor observed, between Peak 1 and the chloride concentration in the seawater. This further discourages the use of gold electrodes for the quantification of chloride in seawater. No clear feature for the oxidation of bromide is visible in any of the voltammograms recorded despite the difference in bromide concentrations. This likely reflects the tiny bromide concentration in comparison with the chloride levels so that any bromide signal is masked by the chloride response. The shoulder noted on Peak 1 is ascribed in the literature to the onset of partial passivation [67,68,71,73], not to bromide oxidation, but in either case, is too ill-defined to be analytically useful.

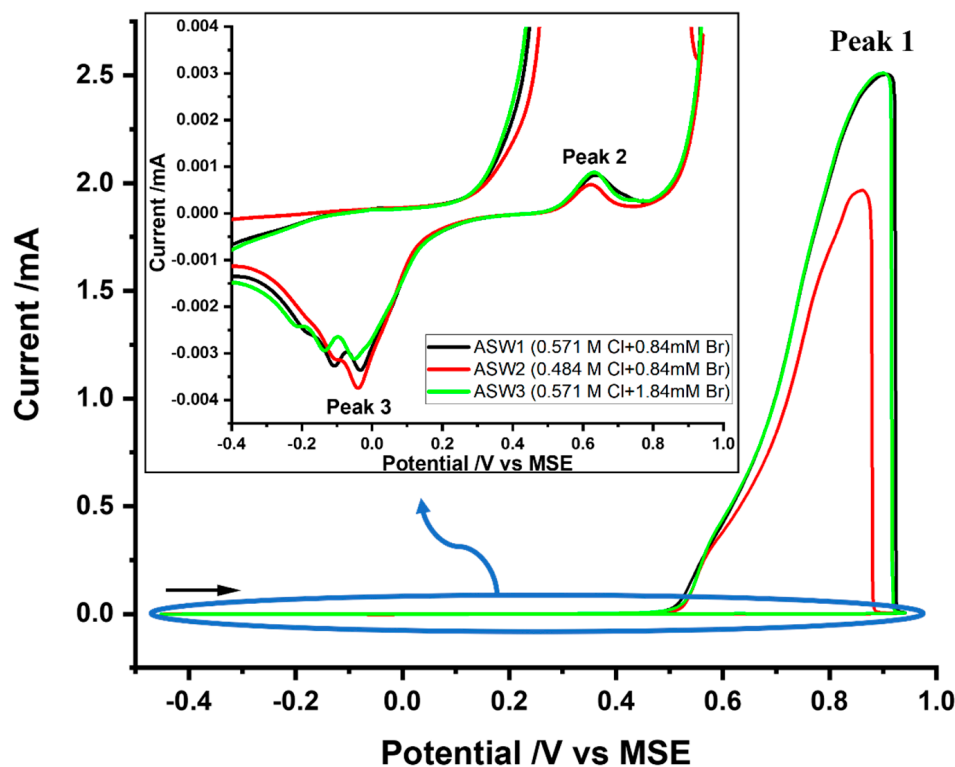


Figure 1. Cyclic voltammograms measured at a scan rate of 20 mV s^{-1} using the Au macro-electrode in degassed ASW1 which contains 0.571 M chloride and 0.84 mM bromide (black line); ASW2 contains 0.484 M chloride and 0.84 mM bromide (red line) and ASW3 contains 0.571 M chloride and 1.84 mM bromide (green line). The start potential is -0.45 V vs. MSE , and the stopping potential is 0.94 V vs. MSE . Insert: an enlarged CV focusing on the reactivation and reduction peaks.

To summarize, the dissolution and passivation of a Au electrode in artificial seawater were inferred from observations in pure chloride and bromide solutions. It is concluded that a gold electrode is unsuitable for use as a Cl^- and/or Br^- sensor.

3.2. Cyclic Voltammetry at Glassy Carbon and Platinum Electrodes in ASW

Next, cyclic voltammetry of ASW using a glassy carbon electrode (GCE) and a Pt electrode was investigated, building on an earlier report [57]. Cyclic voltammograms were first recorded with a scan rate of 100 mVs^{-1} using either the Pt electrode or the GCE in degassed ASW (see Figure 2a). For the Pt electrode, the potential sweep started at -0.45 V vs. MSE , and swept towards 1.2 V before returning to -0.45 V (red line). For the GCE, the voltammogram started at the same potential of -0.45 V vs. MSE , followed by an anodic sweep up to 2.0 V followed by a cathodic scan to -1.3 V before a further anodic sweep back to -0.45 V (blue line). The potential ranges were chosen to obtain both forward and reverse peaks of the redox reactions assigned to the analytes, chloride and bromide, as discussed as below, and to explore the anodic potential window before solvent oxidation.

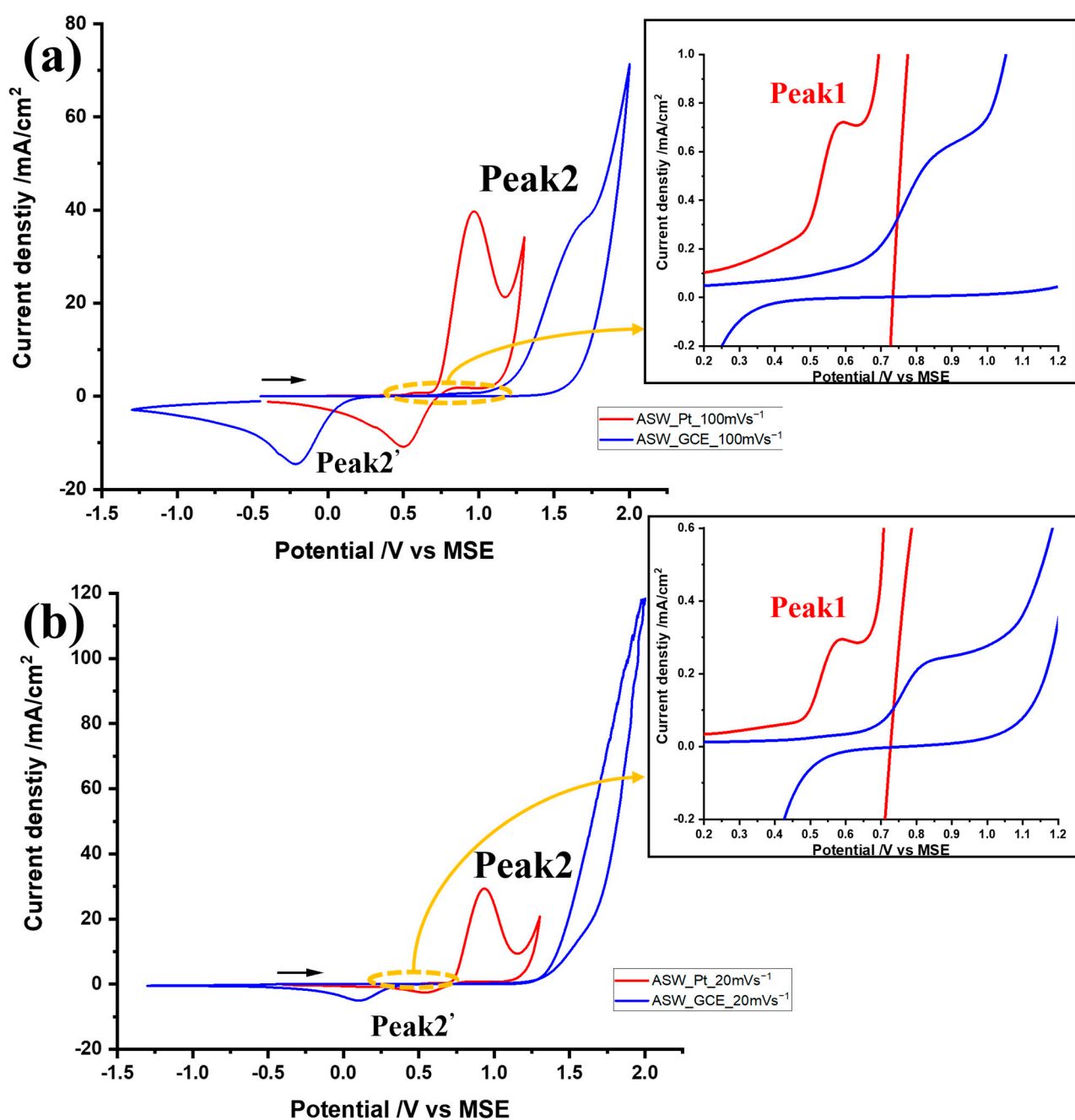


Figure 2. Cyclic voltammograms using a Pt electrode (red) and GCE (blue) in degassed ASW with different scan rates of (a) 100 mVs^{-1} and (b) 20 mVs^{-1} . Insert: expanded bromide oxidation peaks. The start potential was -0.45 V vs. MSE .

The dominant oxidation peak (Peak 2) was observed at 0.94 V vs. MSE using the Pt electrode; the corresponding feature appears as a shoulder on the solvent decomposition at ca. 1.66 V vs. MSE using the GCE. As the insert shows, a first oxidation peak (Peak 1) was recorded at 0.59 V vs. MSE using the Pt electrode and 0.86 V vs. MSE using the GCE. Referring to the previous study [57], Peak 2 is attributed to the oxidation of chloride with the possible formation of hypochlorite/hypochlorous acid (HOCl/OCl^-), and Peak 1 is attributed to bromide oxidation with hypobromous acid (HOBr/OBr^-), which is among the possible products reported by Yu et al. [77]. The Peak 2' corresponds to the reduction of the products from the chloride and bromide oxidation. GC offers a wider anodic potential window compared to platinum.

Inspection of the wave-shapes of the dominant peaks in Figure 1a shows that the redox reaction of chloride is relatively much more electrochemically reversible on Pt than on GC, as evidenced by the reduced peak-to-peak separation between the anodic and cathodic peaks, and also the steepness of the current–voltage curves. The Tafel slopes were calculated as described in Supporting Information Section S2 [78–81], with the β value for chloride oxidation being 0.64 at the Pt electrode and 0.22 at the GCE. To confirm this relative assessment of reversibility, cyclic voltammetry, with the same potential window for each electrode, was conducted at a slower scan rate of 20 mVs^{−1} (see Figure 2b). For the Pt electrode (red line), the oxidation of bromide (Peak 1) occurred at 0.59 V vs. MSE and chloride oxidation appeared at 0.94 V vs. MSE (Peak 2), followed by a reduction peak at 0.60 V vs. MSE (Peak 2′). In contrast to the voltammogram of the Pt electrode that only showed insignificant peak shifts when the slower scan rate was applied, that obtained at the GCE showed more noticeable changes (blue line), with the peak-to-peak separation decreasing with scan rate, as particularly seen in the peak potential of Peak 2′. Again, the chloride oxidation of Peak 2 is heavily merged with the solvent decomposition and is not resolved from it. These observations suggest that chloride oxidation is electrochemically irreversible in GC but nearly reversible in Pt.

From the above, it can be seen that Pt and GC electrodes show signals of similar magnitude (current density) for chloride oxidation, but the proximity of the voltametric feature to solvent decomposition prevented the identification of a clear peak at the GC electrode, especially at lower scan rates. For the Pt electrode, a plot of the peak current of chloride oxidation obtained experimentally vs. the square root of the scan rate is shown in Figure 3, where it is compared with the diffusion-controlled response calculated using the Randles–Ševčík equation (Equation (7)) for an irreversible one-electron reaction at 298K:

$$I_p = 2.99 \times 10^5 \sqrt{\beta} (D_{Cl^-})^{1/2} C_{Cl^-} A v^{1/2} \quad (7)$$

where the concentration of chloride in ASW is $C_{Cl^-} = 0.56 \times 10^{-3} \text{ mol cm}^{-3}$ [75], the diffusion coefficient of chloride (D_{Cl^-}) in seawater is $1.8 \times 10^{-5} \text{ cm}^2/\text{s}$ [82] and the area (A) of the electrode is 0.02 cm^2 . The transfer coefficient reported above ($\beta = 0.64$) was used. Figure 3 shows a gradual increase in signal with scan rate, but less than expected for a fully diffusional signal. This likely reflects the extremely high concentration of chloride, resulting in currents in the order of milliamperes, where the oxidation rate may be largely limited by the availability of adsorption sites for the likely chlorine atom intermediate, together with a contribution to the current from migration effects, since electrolysis is essentially ‘unsupported’.

In the case of bromide, signals are seen at less positive potentials for both electrode materials, but these are much smaller in size relative to the chloride peak reflecting the relative concentrations of the two species. Importantly, as the GCE leads to the bromide oxidation peak being more separated from the onset of chloride oxidation compared to the Pt electrode, this gives a superior resolution for Br[−] detection. Meanwhile, a Pt electrode is preferable for chloride detection, with a well-defined chloride oxidation peak and a greater degree of electrochemical reversibility. Thus, the use of a GCE for the analysis of bromide ions in ASW was explored further, whilst the merits of using a Pt electrode for the quantitative analysis of chloride were also investigated. In the following sections, the behaviour of the GCE will be discussed first, followed by that of the Pt electrode.

3.3. Analysis of Bromide at the Glassy Carbon Electrode

In this section, a GCE is briefly assessed for the oxidation of bromide ions in ASW from an analytical perspective. The study was carried out via cyclic voltammetry with different scan rates of 20, 50, 100, 200 and 400 mVs^{−1}, where the sweep of potential started at -0.45 V vs. MSE , and then, swept towards 1.1 V before returning to -0.45 V . The voltammograms are shown in Figure 4, where the two features identified above were again observed, namely, bromide oxidation and the corresponding reduction. Although these

increased with increasing scan rate, the oxidation of bromide cannot be distinguished from the oxidation peak of chloride, which is also found to interfere with the oxygen evolution reaction (OER). In addition to the proximity to chloride oxidation and the OER, the presence of a pre-wave (see later) also prevented quantitative Tafel analysis and the application of the Randles–Ševčík equation. Attempts were made to increase its resolution using square wave voltammetry but, as reported Supporting Information Section S3, these were unsuccessful. Our attention therefore returned to the cyclic voltammetric data and a standard addition approach was adopted [58].

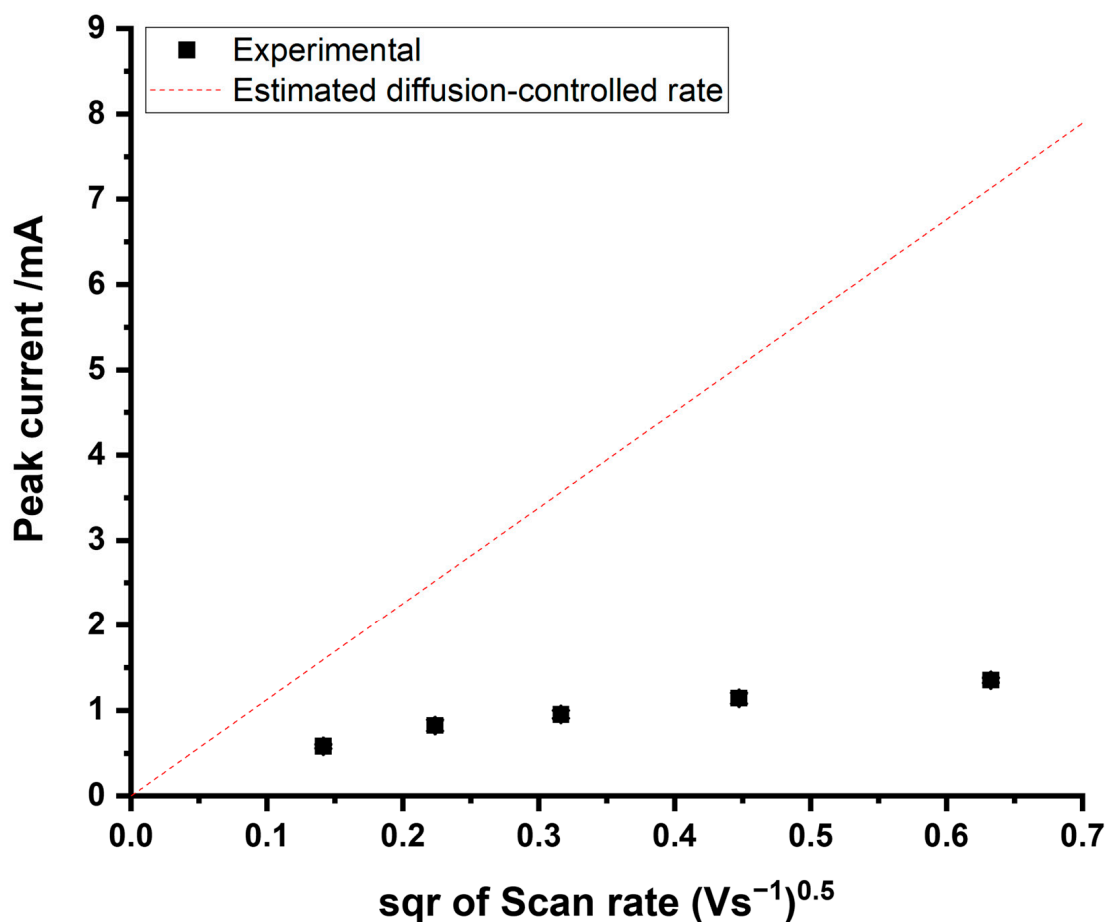


Figure 3. The plot of the peak current against the square root of the scan rate. Experimental data: black squares. Estimated diffusion-controlled rate (red dotted line).

As shown in Figure 5a, voltammograms were recorded with a scan rate of 100 mVs^{-1} representing a compromise between a larger Faradaic signal and excessive capacitive charging. The potential scan of the voltammograms started at a potential of -0.45 V vs. MSE , with a return potential of 1.1 V , before returning -0.45 V . Figure 5 shows that, as expected, Peak 1 increases with the addition of bromide, whilst there is a clear pre-wave to Peak 1 at potentials of around 0.54 V vs. MSE . Additions of $0.2\text{--}1.0 \text{ mM KBr}$ to the ASW solutions were conducted. The measurements taken with each addition were repeated three times. To analyse the data, the oxidation peak currents of Peak 1 were recorded. Because of the pre-wave to Peak 1, a baseline correction was required for each measurement, examples of which are shown in Figure S5, Supporting Information Section S4. Figure 4b shows a plot of peak current against the concentration of bromide added to the original ASW, indicating good linearity ($R^2 = 0.996$). As the intercept on the x-axis corresponds with the unknown initial concentration of the analyte [58], the intercept of $-0.84 \pm 0.06 \text{ mM}$ shows excellent agreement with the known bromide concentration (0.84 mM [75]) in the ASW samples.

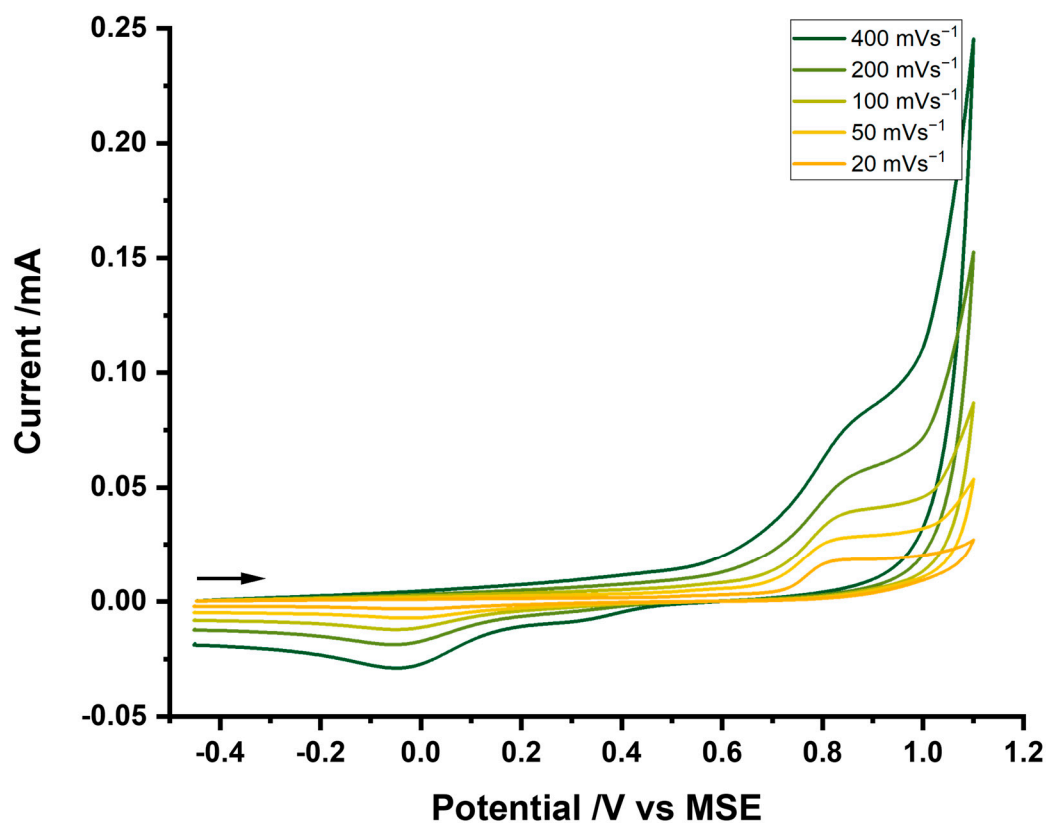


Figure 4. Cyclic voltammograms recorded at the GCE in degassed ASW at variable scan rates of 20, 50, 100, 200 and 400 mV s^{-1} .

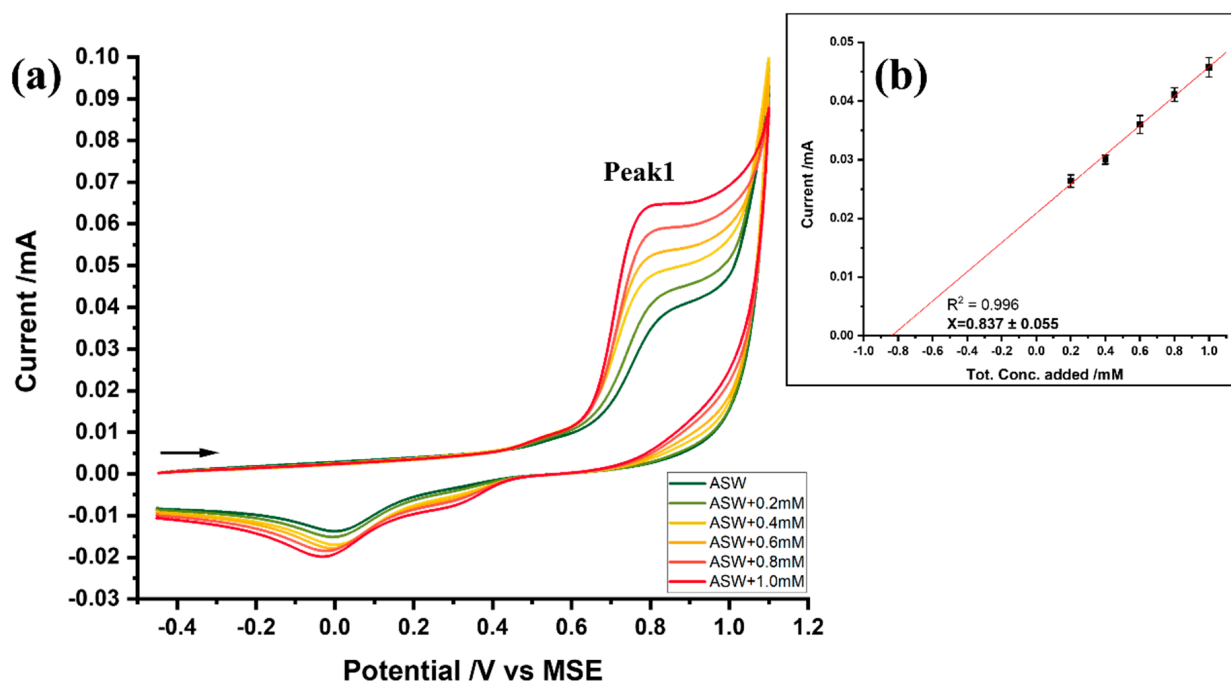


Figure 5. (a) Cyclic voltammograms recorded at the GCE in degassed ASW and with standard additions at a scan rate of 100 mV s^{-1} . The start potential was -0.45 V vs. MSE . (b) Graphical analysis of standard additions.

Although this suggests the possibility of using a GCE as a bromide sensor, the proximity of bromide oxidation to that of chloride, and of the OER to Peak 2, and the challenges of

making a suitable and unambiguous baseline correction, make this method less attractive than the determination of bromide using a platinum electrode [57], where these problems are mitigated.

We next consider the analysis of chloride in seawater using Pt.

3.4. Analysis of Chloride at the Platinum Electrode

As discussed previously, for chloride detection, Pt is a more suitable electrode material compared to GC due to the distinct peak for chloride oxidation and the higher level of electrochemical reversibility. Therefore, the quantitative analysis of chloride in ASW using a Pt electrode was investigated next. This study was conducted in ASW with six levels of chloride concentration from 0.484 M to 0.593 M, while the other components followed a standard recipe (Table 2 [75,76]). Note that the detection range was expanded slightly beyond the recommended range (from 32 g kg⁻¹ to 37 g kg⁻¹) to a range of 31 g kg⁻¹ to 38 g kg⁻¹ to obtain a potentially wider concentration range of the analyte [10]. To achieve a best-resolved chloride signal, square wave voltammetry was implemented, with the corresponding parameters optimised as shown in Supporting Information Section S5. A step potential of 1 mV, a frequency of 5 Hz and an amplitude of 50 mV were then employed. To obtain electroanalytical responses, the potential sweep started from -0.45 V and stopped at 1.25 V vs. MSE for oxidative scanning in six ASW solutions of variable chloride content in the range specified above (Figure 6).

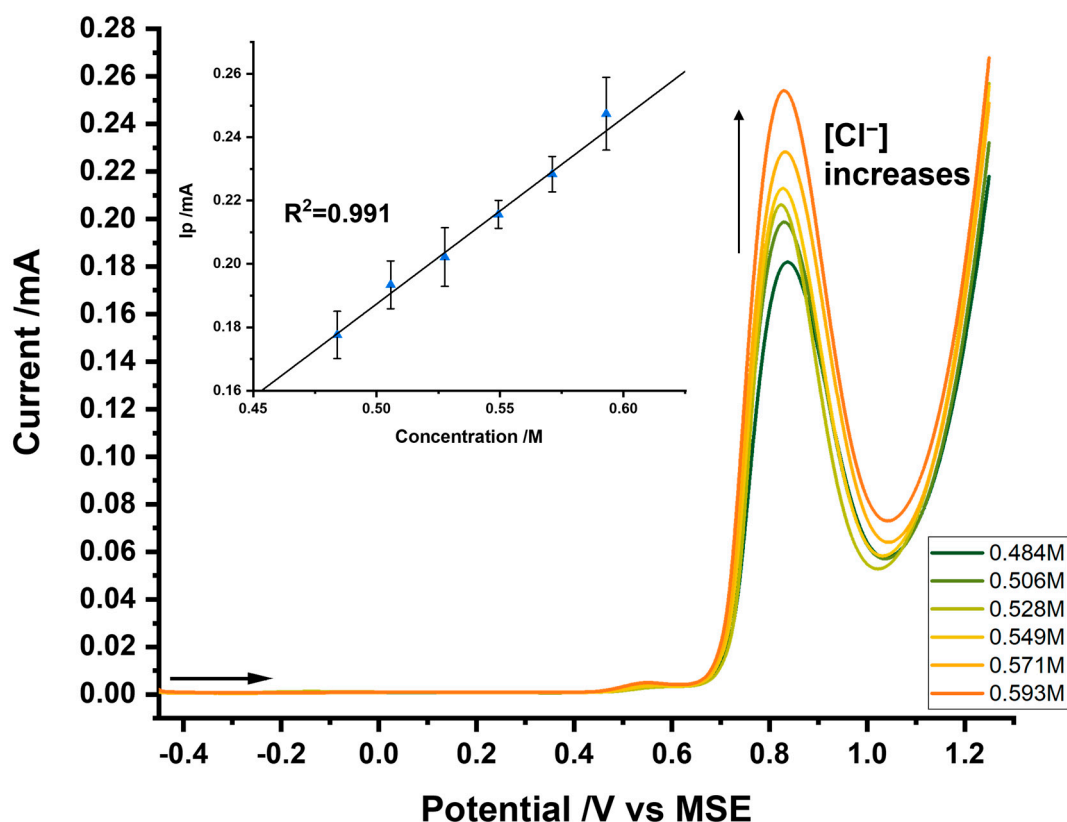


Figure 6. Square wave voltammograms (step potential: 1 mV, frequency: 5 Hz, and amplitude: 50 mV) recorded at the Pt electrode in degassed ASW with various chloride concentrations ranging from 0.484M to 0.593M. See text for details of the scan range and the start potential. The inset shows the calibration curve of the chloride oxidation peak height against chloride concentrations, with a regression coefficient R^2 of 0.991. Each data point consists of 3 repeats.

The dominant chloride oxidation peak was recorded at 0.83 V vs. MSE. To analyse the data, the oxidation peak currents of the chloride were measured. A plot of the peak current against the chloride concentration in the ASW samples is shown in the inset of Figure 6.

The peak height increased linearly in the concentration range of chloride studied (from 0.484 M to 0.593 M). The best-fit line ($R^2 = 0.991$) was determined as follows:

$$I_p = 0.587[\text{Cl}^-] - 0.106 \quad (8)$$

where I_p is the peak current (mA) of chloride oxidation and $[\text{Cl}^-]$ is the concentration (M) of chloride in ASW.

3.5. Real Sample Analysis

To investigate the method in authentic seawater, an analysis of two different samples was performed. Ion chromatography measurements were first made for the chloride concentration of the two samples, with a result of 0.579 ± 0.004 M for sample 1 and 0.580 ± 0.001 M for sample 2. The concentrations of chloride obtained via IC were then compared as follows, with the values measured electrochemically, and as performed in ASW via SWV with optimal parameters: a step potential of 1 mV, a frequency of 5 Hz and an amplitude of 50 mV. As shown in Figure 7, voltammograms were conducted, starting at a potential of -0.45 V and stopping at 1.25 V vs. MSE, to record the chloride oxidation signal. The oxidation peaks of chloride in the three solutions all appear at 0.83 V vs. MSE, with no additional features being observed in the real samples. With the three measurements, the average oxidation peak currents of the chloride obtained in sample 1 and sample 2 were recorded and analysed using the calibration made above in ASW (Equation (8)). The electrochemically measured chloride concentrations in sample 1 and sample 2 are 0.579 ± 0.003 and 0.581 ± 0.005 , respectively. The developed electrochemical analysis resulted in good agreement with IC.

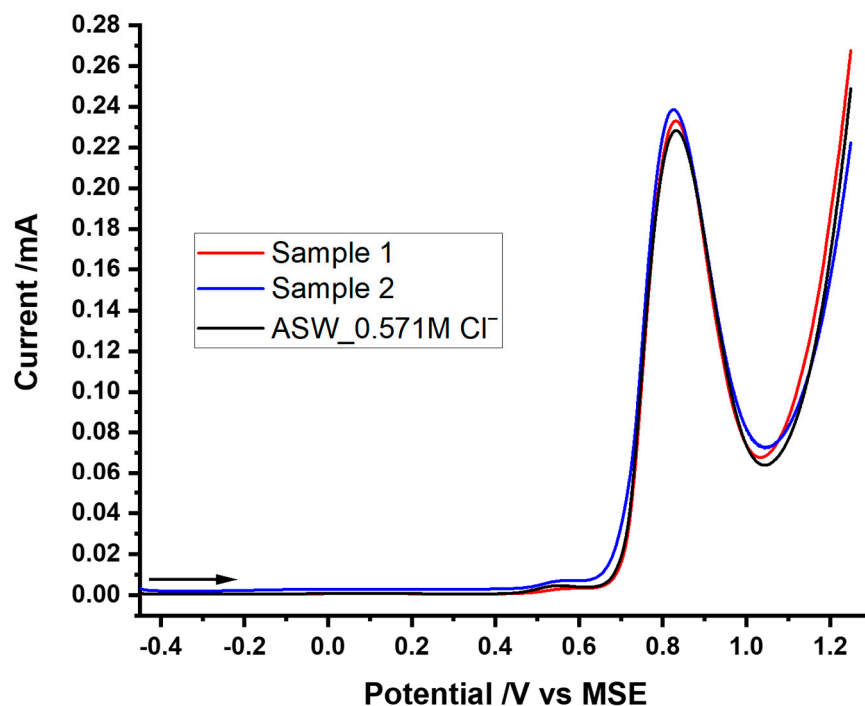


Figure 7. Square wave voltammograms (step potential: 1 mV, frequency: 5 Hz and amplitude: 50 mV) recorded at the Pt electrode in degassed sample 1 (red line), sample 2 (blue line) and ASW with a chloride concentration of 0.571 M (black line). See text for details of the scan range and the start potential.

4. Conclusions

In conclusion, three electrodes, made of Au, glassy carbon and Pt, were investigated for the analysis of Cl^- and/or Br^- in seawater. First, the dissolution and passivation of a Au electrode in ASW, which has a high chloride concentration, indicated that gold

was an unsuitable electrode material. This agrees with independent studies on pure chloride and bromide solutions. For GC, while the proximity of the voltametric feature to solvent decomposition (OER) prevented the identification of a clear chloride oxidation peak, the poorly resolved bromide signal from the chloride oxidation and the OER, and the challenges of making an appropriate baseline correction, make the material less attractive than using platinum for chloride detection in both ASW and NSW using SWV. The results measured electrochemically in two real samples show a good match with those measured independently via ion chromatography. Platinum electrodes are also recommended for bromide detection using a previously developed method for seawater [57].

Supplementary Materials: The following supporting information can be downloaded at: <https://www.mdpi.com/article/10.3390/chemosensors11050297/s1>. References [78–81] are cited in the Supplementary Information Section S2: Calculation of Transfer Coefficients for the Chloride Oxidation from Tafel Analysis.

Author Contributions: Y.C.: validation, formal analysis, investigation, writing—original draft and visualisation; R.G.C.: writing—review and editing, supervision, project administration, funding acquisition, conceptualisation, methodology and resources. All authors have read and agreed to the published version of the manuscript.

Funding: This research received no external funding.

Institutional Review Board Statement: Not applicable.

Informed Consent Statement: Not applicable.

Data Availability Statement: The study did not report any data.

Conflicts of Interest: The authors declare that they have no known competing financial interests or personal relationships that could have appeared to influence the work reported in this paper.

References

1. Water Scarcity. Available online: <https://www.unwater.org/water-facts/water-scarcity> (accessed on 14 March 2023).
2. Spellman, F.R. *The Handbook of Nature*; Bernan Press: Lanham, MD, USA, 2019.
3. Bint El Hassan, H.E.S.; Guerrier, D.; Closas, A.; Demilecamps, C.; kassim, Y.; Lacirignola, C.; Lamaddalena, N.; Mateo-Sagasta, J.; Rivera, N. *Water Around the Mediterranean*; The Center for Mediterranean Integration (CMI): Marseille, France, 2018.
4. Pérez-González, A.; Urtiaga, A.M.; Ibáñez, R.; Ortiz, I. State of the art and review on the treatment technologies of water reverse osmosis concentrates. *Water Res.* **2012**, *46*, 267–283. [[CrossRef](#)] [[PubMed](#)]
5. Kim, D.H. A review of desalting process techniques and economic analysis of the recovery of salts from retentates. *Desalination* **2011**, *270*, 1–8. [[CrossRef](#)]
6. Wallace, W.J. *The Development of the Chlorinity/Salinity Concept in Oceanography*; Elsevier Science Ltd.: New York, NY, USA, 1974.
7. Millero, F.J.; Feistel, R.; Wright, D.G.; McDougall, T.J. The composition of Standard Seawater and the definition of the Reference-Composition Salinity Scale. *Deep Sea Res.* **2008**, *55*, 50–72. [[CrossRef](#)]
8. Stewart, R.H. *Introduction to Physical Oceanography*; Department of Oceanography, Texas A&M University: College Station, TX, USA, 2008.
9. Shumway, S.E. Effect of salinity fluctuation on the osmotic pressure and Na⁺, Ca²⁺ and Mg²⁺ ion concentrations in the hemolymph of bivalve molluscs. *Mar. Biol.* **1977**, *41*, 153–177. [[CrossRef](#)]
10. Guo, Y.; Compton, R.G. A bespoke chloride sensor for seawater: Simple and fast with a silver electrode. *Talanta* **2021**, *232*, 122502. [[CrossRef](#)]
11. Yamamoto, M. Stimulation of elemental mercury oxidation in the presence of chloride ion in aquatic environments. *Chemosphere* **1996**, *32*, 1217–1224. [[CrossRef](#)]
12. Levard, C.; Mitra, S.; Yang, T.; Jew, A.D.; Badireddy, A.R.; Lowry, G.V.; Brown, G.E., Jr. Effect of Chloride on the Dissolution Rate of Silver Nanoparticles and Toxicity to *E. coli*. *Environ. Sci. Technol.* **2013**, *47*, 5738–5745. [[CrossRef](#)] [[PubMed](#)]
13. Batchelor-McAuley, C.; Tschulik, K.; Neumann, C.; Laborda, E.; Compton, R. Why are silver nanoparticles more toxic than bulk silver? Towards understanding the dissolution and toxicity of silver nanoparticles. *Int. J. Electrochem. Sci.* **2014**, *9*, 1132–1138.
14. Gilberg, M.R.; Seeley, N.J. The identity of compounds containing chloride ions in marine iron corrosion products: A critical review. *Stud. Conserv.* **1981**, *26*, 50–56. [[CrossRef](#)]
15. Otieno, M.; Beushausen, H.; Alexander, M. Chloride-induced corrosion of steel in cracked concrete—Part I: Experimental studies under accelerated and natural marine environments. *Cem. Concr. Res.* **2016**, *79*, 373–385. [[CrossRef](#)]
16. Downs, A.J.; Adams, C.J. *The Chemistry of Chlorine, Bromine, Iodine and Astatine: Pergamon Texts in Inorganic Chemistry, Volume 7*; Elsevier: Amsterdam, The Netherlands, 2017; Volume 7.

17. Leri, A.C.; Hakala, J.A.; Marcus, M.A.; Lanzirrotti, A.; Reddy, C.M.; Myneni, S.C.B. Natural organobromine in marine sediments: New evidence of biogeochemical Br cycling. *Glob. Biogeochem. Cycles* **2010**, *24*, 1–15. [[CrossRef](#)]
18. Pilson, M.E. *An Introduction to the Chemistry of the Sea*; Cambridge University Press: Cambridge, UK, 2012.
19. Gribble, G.W. Amazing Organohalogens: Although best known as synthetic toxicants, thousands of halogen compounds are, in fact, part of our natural environment. *Am. Sci.* **2004**, *92*, 342–349. [[CrossRef](#)]
20. Dorji, P.; Kim, D.I.; Hong, S.; Phuntsho, S.; Shon, H.K. Pilot-scale membrane capacitive deionisation for effective bromide removal and high water recovery in seawater desalination. *Desalination* **2020**, *479*, 114309. [[CrossRef](#)]
21. Lewis, E.L. The practical salinity scale of 1978 and its antecedents. *Mar. Geod.* **1982**, *5*, 350–357. [[CrossRef](#)]
22. Lagerloef, G.S.; Swift, C.T.; Le Vine, D.M. Sea surface salinity: The next remote sensing challenge. *Oceanog.* **1995**, *8*, 44–50. [[CrossRef](#)]
23. Anfält, T.; Twengström, S. The determination of bromide in natural waters by flow injection analysis. *Anal. Chim. Acta* **1986**, *179*, 453–457. [[CrossRef](#)]
24. Vengosh, A.; Pankratov, I. Chloride/Bromide and Chloride/Fluoride Ratios of Domestic Sewage Effluents and Associated Contaminated Ground Water. *Ground Water* **1998**, *36*, 815–824. [[CrossRef](#)]
25. Morgan, J.J.; Stumm, W. *Aquatic Chemistry: An Introduction Emphasizing Chemical Equilibria in Natural Waters*; John Wiley & Sons: New York, NY, USA, 1981.
26. Salameh, E.; Tarawneh, A.; Al-Raggad, M. Origin of high bromide concentration in the water sources in Jordan and in the Dead Sea water. *Arabian J. Geosci.* **2016**, *9*, 414. [[CrossRef](#)]
27. Jain, A.; Chaurasia, A.; Sahasrabudhhey, B.; Verma, K.K. Determination of bromide in complex matrices by pre-column derivatization linked to solid-phase extraction and high-performance liquid chromatography. *J. Chromatogr. A* **1996**, *746*, 31–41. [[CrossRef](#)]
28. Borges, E.P.; Lavorante, A.F.; Reis, B.F.d. Determination of bromide ions in seawater using flow system with chemiluminescence detection. *Anal. Chim. Acta* **2005**, *528*, 115–119. [[CrossRef](#)]
29. Grasshoff, K.; Wenck, A. A modern version of the Mohr-Knudsen titration for the chlorinity of sea water. *ICES Mar. Sci. Symp.* **1972**, *34*, 522–528. [[CrossRef](#)]
30. Hong, T.-K.; Kim, M.-H.; Czae, M.-Z. Determination of chlorinity of water without the use of chromate indicator. *Int. J. Anal. Chem.* **2010**, *2010*, 602939. [[CrossRef](#)] [[PubMed](#)]
31. Reitemeier, R. Semimicroanalysis of saline soil solutions. *Ind. Eng. Chem. Anal. Ed.* **1943**, *15*, 393–402. [[CrossRef](#)]
32. Reeburgh, W.S.; Carpenter, J.H. Determination of chlorinity using A differential potentiometric. *Limnol. Oceanogr.* **1964**, *9*, 589–591. [[CrossRef](#)]
33. Clesceri, L.S.; Greenberg, A.E.; Eaton, A.D. *Standard Methods for the Examination of Water and Wastewater*, 20th ed.; APHA American Public Health Association: Washington, DC, USA, 1998.
34. Willard, H.H.; Merritt, L.L., Jr.; Dean, J.A.; Settle, F.A., Jr. *Instrumental Methods of Analysis*, 7th ed.; Wadsworth Publishing Company: Belmont, CA, USA, 1988.
35. Lewis, E. The practical salinity scale 1978 and its antecedents. *IEEE J. Ocean.* **1980**, *5*, 3–8. [[CrossRef](#)]
36. Lewis, E.; Perkin, R. The Practical Salinity Scale 1978: Conversion of existing data. *Deep Sea Res.* **1981**, *28*, 307–328. [[CrossRef](#)]
37. Unesco. *Tenth Report of the Joint Panel on Oceanographic Tables and Standards*; Unesco Division of Marine Sciences: Sidney, BC, Canada, 1980.
38. Uraisin, K.; Takayanagi, T.; Oshima, M.; Nacapricha, D.; Motomizu, S. Kinetic-spectrophotometric method for the determination of trace amounts of bromide in seawater. *Talanta* **2006**, *68*, 951–956. [[CrossRef](#)]
39. Jones, D.R. Applying the phenol red colorimetric method for bromide analysis to reducing waters. *Talanta* **1993**, *40*, 43–51. [[CrossRef](#)]
40. Anagnostopoulou, P.I.; Koupparis, M.A. Automated flow-injection phenol red method for determination of bromide and bromide salts in drugs. *Anal. Chem.* **1986**, *58*, 322–326. [[CrossRef](#)]
41. Emaus, W.J.M.; Henning, H.J. Determination of bromide in sodium chloride matrices by flow-injection analysis using blank peak elimination and kinetic discrimination. *Anal. Chim. Acta* **1993**, *272*, 245–250. [[CrossRef](#)]
42. Uraisin, K.; Nacapricha, D.; Lapanantnoppakhun, S.; Grudpan, K.; Motomizu, S. Determination of trace amounts of bromide by flow injection/stopped-flow detection technique using kinetic-spectrophotometric method. *Talanta* **2005**, *68*, 274–280. [[CrossRef](#)] [[PubMed](#)]
43. Yonehara, N.; Chaen, S.-i.; Tomiyasu, T.; Sakamoto, H. Flow injection-spectrophotometric determination of trace amounts of bromide by its catalytic effect on the 4,4'-bis(dimethylamino)diphenylmethane-chloramine T reaction. *Anal. Sci.* **1999**, *15*, 277–281. [[CrossRef](#)]
44. Shishehbori, M.R.; Elah, J.R. Kinetic spectrophotometric method For trace amounts determination of bromide in pharmaceutical samples using Janus Green-Bromate system. *Int. J. Ind. Chem.* **2011**, *2*, 27–32.
45. Sheibani, A.; Shishehbore, M.R.; Ardakani, Z.T. Kinetic spectrophotometric determination of bromide in clidinium-c drug. *Chin. Chem. Lett.* **2011**, *22*, 595–598. [[CrossRef](#)]
46. Akaiwa, H.; Kawamoto, H.; Osumi, M. Simultaneous determination of bromide and chloride in natural waters by ion-exchange chromatography and direct potentiometry with an ion-selective electrode. *Talanta* **1982**, *29*, 689–690. [[CrossRef](#)]

47. Seefeld, S.; Baltensperger, U. Determination of bromide in snow samples by ion chromatography with electrochemical detection. *Anal. Chim. Acta* **1993**, *283*, 246–250. [[CrossRef](#)]
48. Fabre, H.; Blanchin, M.D.; Bosc, N. Capillary electrophoresis for the determination of bromide, chloride and sulfate as impurities in calcium acamprostate. *Anal. Chim. Acta* **1999**, *381*, 29–37. [[CrossRef](#)]
49. Stålberg, O.; Sander, K.; Sängler-van de Griend, C. The determination of bromide in a local anaesthetic hydrochloride by capillary electrophoresis using direct UV detection. *J. Chromatogr. A* **2002**, *977*, 265–275. [[CrossRef](#)]
50. Pascali, J.P.; Trettene, M.; Bortolotti, F.; Paoli, G.d.; Gottardo, R.; Tagliaro, F. Direct analysis of bromide in human serum by capillary electrophoresis. *J. Chromatogr. B* **2006**, *839*, 2–5. [[CrossRef](#)]
51. Fukushi, K.; Watanabe, K.; Takeda, S.; Wakida, S.-I.; Yamane, M.; Higashi, K.; Hiroy, K. Determination of bromide ions in seawater by capillary zone electrophoresis using diluted artificial seawater as the buffer solution. *J. Chromatogr. A* **1998**, *802*, 211–217. [[CrossRef](#)]
52. Kocatürk, N.; Öztekin, N.; Bedia Erim, F. Direct determination of bromide ions in seawater by capillary zone electrophoresis using polyethyleneimine-coated capillaries. *Anal. Bioanal. Chem.* **2003**, *377*, 1207–1211. [[CrossRef](#)]
53. Rechnitz, G.A.; Kresx, M.R. Potentiometric measurements with chloride-sensitive and bromide-sensitive membrane electrodes. *Anal. Chem.* **1966**, *38*, 1786–1788. [[CrossRef](#)]
54. Zahran, E.M.; Hua, Y.; Li, Y.; Flood, A.H.; Bachas, L.G. Triazolophanes: A new class of halide-selective ionophores for potentiometric sensors. *Anal. Chem.* **2010**, *82*, 368–375. [[CrossRef](#)] [[PubMed](#)]
55. Isildak, Ö.; Özbek, O.; Yigit, K. A bromide-selective PVC membrane potentiometric sensor. *Bulg. Chem. Commun.* **2020**, *52*, 448–452. [[CrossRef](#)]
56. Vlascici, D.; Plesu, N.; Fagadar-Cosma, G.; Lascu, A.; Petric, M.; Crisan, M.; Belean, A.; Fagadar-Cosma, E. Potentiometric sensors for iodide and bromide based on Pt(II)-Porphyrin. *Sensors* **2018**, *18*, 2297. [[CrossRef](#)]
57. Chen, Y.; Compton, R.G. A bespoke reagent-free amperometric bromide sensor for seawater. *Talanta* **2023**, *253*, 124019. [[CrossRef](#)]
58. Harris, D.C. *Quantitative Chemical Analysis*; Macmillan: London, UK, 2010.
59. Sekerka, I.; Lechner, J.F. Ion Selective Electrode for Determination of Chloride Ion in Biological Materials, Food Products, Soils, and Waste Water. *J. Assoc. Off. Anal. Chem.* **2020**, *61*, 1493–1495. [[CrossRef](#)]
60. Montemor, M.; Alves, J.; Simoes, A.; Fernandes, J.; Lourenço, Z.; Costa, A.; Appleton, A.; Ferreira, M. Multiprobe chloride sensor for in situ monitoring of reinforced concrete structures. *Cem. Concr. Compos.* **2006**, *28*, 233–236. [[CrossRef](#)]
61. Arai, K.; Kusu, F.; Noguchi, N.; Takamura, K.; Osawa, H. Selective determination of chloride and bromide ions in serum by cyclic voltammetry. *Anal. Biochem.* **1996**, *240*, 109–113. [[CrossRef](#)] [[PubMed](#)]
62. Qin, X.; Wang, H.; Miao, Z.; Wang, X.; Fang, Y.; Chen, Q.; Shao, X. Synthesis of silver nanowires and their applications in the electrochemical detection of halide. *Talanta* **2011**, *84*, 673–678. [[CrossRef](#)]
63. Bujes-Garrido, J.; Izquierdo-Bote, D.; Heras, A.; Colina, A.; Arcos-Martínez, M.J. Determination of halides using Ag nanoparticles-modified disposable electrodes. A first approach to a wearable sensor for quantification of chloride ions. *Anal. Chim. Acta* **2018**, *1012*, 42–48. [[CrossRef](#)]
64. Malongo, T.K.; Patris, S.; Macours, P.; Cotton, F.; Nsangu, J.; Kauffmann, J.-M. Highly sensitive determination of iodide by ion chromatography with amperometric detection at a silver-based carbon paste electrode. *Talanta* **2008**, *76*, 540–547. [[CrossRef](#)]
65. Cunha-Silva, H.; Julia Arcos-Martínez, M. Development of a selective chloride sensing platform using a screen-printed platinum electrode. *Talanta* **2019**, *195*, 771–777. [[CrossRef](#)] [[PubMed](#)]
66. Millero, F.J. The Physical Chemistry of Seawater. *Annu. Rev. Earth Planet. Sci.* **1974**, *2*, 101–150. [[CrossRef](#)]
67. Qi, P.H.; Hiskey, J.B. Electrochemical behavior of gold in iodide solutions. *Hydrometallurgy* **1993**, *32*, 161–179. [[CrossRef](#)]
68. Nicol, M.J. The anodic behaviour of gold. *Gold Bull.* **1980**, *13*, 46–55. [[CrossRef](#)]
69. Nicol, M.J. The anodic behaviour of gold. *Gold Bull.* **1980**, *13*, 105–111. [[CrossRef](#)]
70. Loo, B.H. In situ identification of halide complexes on gold electrode by surface-enhanced Raman spectroscopy. *J. Phys. Chem.* **1982**, *86*, 433–437. [[CrossRef](#)]
71. Gaur, J.; Schmid, G. Electrochemical behavior of gold in acidic chloride solutions. *J. Electroanal. Chem. Interfacial Electrochem.* **1970**, *24*, 279–286. [[CrossRef](#)]
72. Cadle, S.; Bruckenstein, S. A ring-disk study of the effect of trace chloride ion on the anodic behavior of gold in 0.2 M H₂SO₄. *J. Electroanal. Chem. Interfacial Electrochem.* **1973**, *48*, 325–331. [[CrossRef](#)]
73. Nicol, M.J.; Schalch, E. *Reports Nos. 1844 and 1848*; National Institute for Metallurgy: Johannesburg, South Africa, 1976.
74. Heumann, T.; Panesar, H.S. Beitrag zur Frage nach dem Auflösungsmechanismus von Gold zu Chlorkomplexen und nach seiner Passivierung. *Z. Phys. Chem.* **1965**, *2290*, 84–97. [[CrossRef](#)]
75. Morel, F.M.M.; Rueter, J.G.; Anderson, D.M.; Guillard, R.R.L. Aquil: A chemically defined phytoplankton culture medium for trace metal studies. *J. Phycol.* **1979**, *15*, 135–141. [[CrossRef](#)]
76. Price, N.M.; Harrison, G.I.; Hering, J.G.; Hudson, R.J.; Nirel, P.M.; Palenik, B.; Morel, F.M. Preparation and chemistry of the artificial algal culture medium Aquil. *Biol. Oceanogr.* **1989**, *6*, 443–461. [[CrossRef](#)]
77. Yu, J.; Yang, M.; Batchelor-McAuley, C.; Barton, S.; Rickaby, R.E.M.; Bouman, H.A.; Compton, R.G. Rapid Opto-electrochemical Differentiation of Marine Phytoplankton. *ACS Meas. Sci. Au* **2022**, *2*, 342–350. [[CrossRef](#)] [[PubMed](#)]
78. Li, D.; Lin, C.; Batchelor-McAuley, C.; Chen, L.; Compton, R.G. Tafel analysis in practice. *J. Electroanal. Chem.* **2018**, *826*, 117–124. [[CrossRef](#)]

79. Compton, R.G.; Banks, C.E. *Understanding Voltammetry*, 3rd ed.; World Scientific: Singapore, 2018.
80. Guidelli, R.; Compton, R.G.; Feliu, J.M.; Gileadi, E.; Lipkowsky, J.; Schmickler, W.; Trasatti, S. Defining the transfer coefficient in electrochemistry: An assessment (IUPAC Technical Report). *Pure Appl. Chem.* **2014**, *86*, 245–258. [[CrossRef](#)]
81. Guidelli, R.; Compton, R.G.; Feliu, J.M.; Gileadi, E.; Lipkowsky, J.; Schmickler, W.; Trasatti, S. Definition of the transfer coefficient in electrochemistry (IUPAC Recommendations 2014). *Pure Appl. Chem.* **2014**, *86*, 259–262. [[CrossRef](#)]
82. Poisson, A.; Papaud, A. Diffusion coefficients of major ions in seawater. *Marine Chemistry* **1983**, *13*, 265–280. [[CrossRef](#)]

Disclaimer/Publisher’s Note: The statements, opinions and data contained in all publications are solely those of the individual author(s) and contributor(s) and not of MDPI and/or the editor(s). MDPI and/or the editor(s) disclaim responsibility for any injury to people or property resulting from any ideas, methods, instructions or products referred to in the content.